JOURNAL OF VIROLOGY, June 1988, p. 1989–1998
0022-538X/88/061989-10$02.00/0

Vol. 62, No. 6

# RNA Recombination of Murine Coronaviruses: Recombination between Fusion-Positive Mouse Hepatitis Virus A59 and Fusion-Negative Mouse Hepatitis Virus 2

JAMES G. KECK, LISA H. SOE, SHINJI MAKINO, STEPHEN A. STOHLMAN, AND MICHAEL M. C. LAI*

*Departments of Microbiology and Neurology, University of Southern California, School of Medicine, Los Angeles, California 90033*

Received 24 November 1987/Accepted 17 February 1988

**It has previously been shown that the murine coronavirus mouse hepatitis virus (MHV) undergoes RNA recombination at a relatively high frequency in both tissue culture and infected animals. Thus far, all of the recombination sites had been localized at the 5′ half of the RNA genome. We have now performed a cross between MHV-2, a fusion-negative murine coronavirus, and a temperature-sensitive mutant of the A59 strain of MHV, which is fusion positive at the permissive temperature. By selecting fusion-positive viruses at the nonpermissive temperature, we isolated several recombinants containing multiple crossovers in a single genome. Some of the recombinants became fusion negative during the plaque purification. The fusion ability of the recombinants parallels the presence or absence of the A59 genomic sequences encoding peplomers. Several of the recombinants have crossovers within 3′ end genes which encode viral structural proteins, N and E1. These recombination sites were not specifically selected with the selection markers used. This finding, together with results of previous recombination studies, indicates that RNA recombination can occur almost anywhere from the 5′ end to the 3′ end along the entire genome. The data also show that the replacement of A59 genetic sequences at the 5′ end of gene C, which encodes the peplomer protein, with the fusion-negative MHV-2 sequences do not affect the fusion ability of the recombinant viruses. Thus, the crucial determinant for the fusion-inducing capability appears to reside in the more carboxyl portion of the peplomer protein.**

Mouse hepatitis virus (MHV), a member of the coronavirus family, contains a single-stranded RNA genome of plus polarity (22, 41). The virus is enveloped and contains three structural proteins. The nucleocapsid protein (N) is a 60-kilodalton phosphoprotein (36), which complexes with virion genomic RNA to form the helical nucleocapsid (37). Surrounding the nucleocapsid is the viral envelope, which contains two viral glycoproteins, designated E1 and E2 (38). E2 is composed of two 90-kilodalton subunits and constitutes the peplomers on the surface (38, 39). It is essential for viral binding to host cells and, in some strains, for induction of cell fusion (9, 12, 39). E1 is a 23-kilodalton glycoprotein, which interacts with the N protein and may play a role in virus assembly (38, 40).

Upon infection, viral genomic RNA is translated into an RNA-dependent RNA polymerase (6), which transcribes the viral RNA into a full-length minus-stranded RNA (6, 21). Subsequently, genomic RNA and six subgenomic mRNAs are transcribed from this minus-stranded template (6, 7). These mRNAs contain a 3′ nested-set structure, in which each mRNA contains a 5′ unique translatable sequence and all the sequences of the next smaller mRNAs (18, 26). Each genomic and subgenomic mRNA also contains a 72-nucleotide leader sequence (16, 19, 35), which is derived from the 5′ end of the genome by a unique discontinuous transcription mechanism; i.e., a free leader RNA serves as a primer for subgenomic mRNA transcription (3). The two smallest mRNAs, mRNAs 6 and 7, representing the 3′ end of the genome, encode the E1 and N proteins, respectively, whereas the middle of the genome, mRNA 3, encodes the E2 protein (25, 34).

Recently, researchers in our laboratory have demonstrated that MHV can undergo RNA recombination at a very high frequency both in tissue culture (14, 17, 28) and in infected animals (13). Recombination occurs at such a high frequency that when two selection markers were used, the recombinants not only contained a crossover between the two markers, but frequently had additional crossovers in other parts of the genome, where no selection pressure was used (27). Thus, many recombinants isolated with only two selectable markers have multiple recombinational events. However, most of the crossover sites in the recombinants isolated thus far are localized in the 5′ half of the genome (14, 17, 28), which encodes viral nonstructural proteins. More recently, by using temperature-sensitive mutants and virus strain-specific monoclonal antibodies, we have succeeded in isolating recombinants with crossovers within the gene encoding the peplomer protein E2 (27). However, we still have not been able to demonstrate recombinational events within the 3′ end genes of the MHV genome. Is there any structural feature in this part of genome, or any constraint on the process of RNA replication, which may prevent RNA recombination? This issue remained to be studied.

So far, all of the recombination studies were carried out between the A59 and JHM strains of MHV. In this report, we studied RNA recombination between A59 and a different strain of MHV, MHV-2. These strains have been shown by serological studies (8) and oligonucleotide fingerprinting analysis (23) to be related. We found that recombination occurred readily between these two MHV strains. Surprisingly, many of these recombinants contain crossovers in the 3′ end genes, which encode the N and E1 proteins, even though no selectable markers were used specifically to isolate recombinants within these regions. We conclude that RNA recombination of MHV could occur almost anywhere in the genome.

* Corresponding author.

## MATERIALS AND METHODS

**Viruses and cells.** The MHV wild-type strain MHV-2 and the temperature-sensitive mutant of A59, LA7, were used in this study. LA7 was isolated by mutagenesis with 5-azacytidine of MHV A59 (J. Egbert et al., unpublished observation). It is RNA positive at the nonpermissive temperature (39°C). The viruses were grown on the murine astrocytoma cell line DBT (11), as described previously (18, 31).

**Isolation of recombinants.** MHV-2 and LA7 were adsorbed to monolayer cultures of DBT cells at a multiplicity of infection of 6 and incubated at 37°C for 1 h. After adsorption, virus was removed and replaced with Dulbecco modified Eagle essential minimal medium containing 10% fetal calf serum, and the mixture was incubated at 39°C. At 12.5 h postinfection, medium containing the virus progeny was harvested. The virus progeny was amplified by passaging in DBT cells twice under the same culture conditions. Serial dilutions of virus samples were plaqued on 100-mm plates of DBT cells for plaque purification. Plaques were examined after incubation at 39°C for 2 days. Fusion-positive plaques were isolated and were further plaque purified four times to eliminate the MHV-2 contamination. The plaque-purified viruses were then used for biochemical studies.

**Radiolabeling and isolation of virion genomic and intracellular RNAs.** Genomic RNA was labeled with $^{32}P_i$ as previously described (17). Briefly, DBT cells were infected with viruses at a multiplicity of infection of 1 and incubated at 37°C for 1 h. The inoculum was removed and replaced with phosphate-free Dulbecco modified Eagle essential minimal medium. At 2 h later, $^{32}P_i$ (200 μCi/ml) was added. At 100% cytopathic effect the medium was harvested, and the virus was purified by sedimentation on continuous 20 to 60% (wt/wt) sucrose gradients. The virus band was collected and pelleted by centrifugation at 27,000 rpm for 4 h in a Beckman SW28.1 rotor. RNA was extracted with phenol-chloroform and precipitated with ethanol as described previously (22).

Intracellular viral RNA was labeled and harvested as previously described (30, 31). Briefly, DBT cells were treated with actinomycin D (2.5 μg/ml) for 1 h prior to being labeled. $^{32}P_i$ (200 μCi/ml) was added at 4 h postinfection, and the cells were harvested at 8 h postinfection for phenol-chloroform extraction.

Genomic and intracellular virus-specific RNAs were separated by electrophoresis on 1% agarose gels (30). The RNA was identified by autoradiography and eluted from the gel by the method of Langridge et al. (24).

**Two-dimensional RNase $T_1$-oligonucleotide fingerprints.** The $^{32}P$-labeled RNA was digested with RNase $T_1$ and fingerprinted as described previously (18, 31). The first-dimension fingerprinting was performed on 10% polyacrylamide–0.125% bisacrylamide gel slabs in citrate buffer (pH 3.3)–6 M urea. Electrophoresis was done for 4 h at 750 V. The second-dimension fingerprinting was performed on 22% polyacrylamide–0.15% bisacrylamide gel slabs in Tris-borate buffer (pH 8.0) at 700 V for 16 h. After electrophoresis, the fingerprints were exposed to an X-ray film with an intensifying screen at 4°C.

**Base composition analysis of oligonucleotides.** The RNase $T_1$-resistant oligonucleotides identified by autoradiography were eluted from the gel by incubation in 0.5 M NaCl at room temperature overnight. The oligonucleotides were precipitated in ethanol by using 10 μg of tRNA as carriers and then digested with RNase A (10 μg/ml) for 30 min. The digested RNA was separated by electrophoresis in acetic acid-pyridine buffer at pH 3.5 as described (5, 20). The marker nucleotides were made by digestion of $^{32}P$-labeled total rRNA with both RNase $T_1$ and RNase A and then separated by electrophoresis under the same conditions as used for the other RNA samples.

**Primer extension and sequence analysis of leader RNA.** The sequencing procedure for leader RNA and the primer used were described previously (14, 16). The primer used, 5′-AGGAACAAAAGACAT-3′, is complementary to nucleotides 84 to 98 from the 5′ end of mRNA 7 of MHV A59 (1). The primer was 5′ end labeled with polynucleotide kinase by using [$\gamma$-$^{32}P$]ATP. It was then hybridized to the total intracellular RNA from MHV-infected cells and primer extended with reverse transcriptase as described (16). The primer-extended products were separated by electrophoresis on 12% polyacrylamide gels. The major extended product (98 nucleotides long), which represents the leader sequence on MHV mRNA 7, was eluted and then sequenced by the Maxam-Gilbert chemical sequencing method (32).

**Radiolabeling of viral polypeptides.** Virion and intracellular viral polypeptides were radiolabeled with [$^{35}S$]methionine. For radiolabeling of virion particles, DBT cells were pretreated with methionine-free medium for 2 h prior to infection. After virus adsorption, the virus inoculum was replaced with methionine-free medium containing 15 μCi of [$^{35}S$]methionine per ml. At 14 h postinfection the medium was harvested and the virus particles were purified as described above. The virus pellets were suspended in Laemmli sample buffer (15) before being subjected to electrophoresis. For radiolabeling of intracellular viral polypeptides, the infected cells were incubated with methionine-free medium at 7 h p.i. for 1 h and then pulse-labeled with [$^{35}S$]methionine (50 μCi/ml) for 20 min. After being labeled, the cells were washed with phosphate-buffered saline and then incubated with 0.5% Nonidet P-40 in NTE (0.1 M NaCl, 0.01 M Tris hydrochloride [pH 7.4], 0.001 M EDTA) for 10 min on ice. The resulting lysate was vortexed and then centrifuged at 12,500 × *g* for 5 min. The supernatant was immunoprecipitated with a mouse monoclonal antibody specific for the N protein of MHV (10) and precipitated with *Staphylococcus aureus* Cowan 1. The immunoprecipitate was suspended in Laemmli sample buffer and boiled for 3 min before being subjected to electrophoresis on a polyacrylamide gel.

**Polyacrylamide gel electrophoresis.** Sodium dodecyl sulfate–polyacrylamide slab gel electrophoresis (12.5% polyacrylamide) was performed as described by Laemmli (15). For separation of E1 polypeptides, the gels were run at 50 V for 14 h or until the Coomassie blue reached the bottom of the gel. For separation of intracellular N proteins, the gel was run at 100 V for 14 h. Both gels with fixed in 50% methanol–7% acetic acid, dried, and exposed to Kodak X-ray film at −70°C.

## RESULTS

**Oligonucleotide mapping of the MHV-2 RNA genome.** As we have shown previously, the nature of RNA recombination between two viruses may be unequivocally established by comparing the $T_1$-oligonucleotide fingerprints of parental viruses and progeny viruses (14, 17, 27, 28). To study recombination with MHV-2, we first needed to map the RNase $T_1$-resistant oligonucleotides of MHV-2 genomic RNA. Although MHV-2 genomic RNA has been fingerprinted (23), the locations of the oligonucleotides on the genomic map had not been determined. The oligonucleotide map of MHV-2 was established by oligonucleotide fingerprinting analysis of the genomic RNA and subgenomic

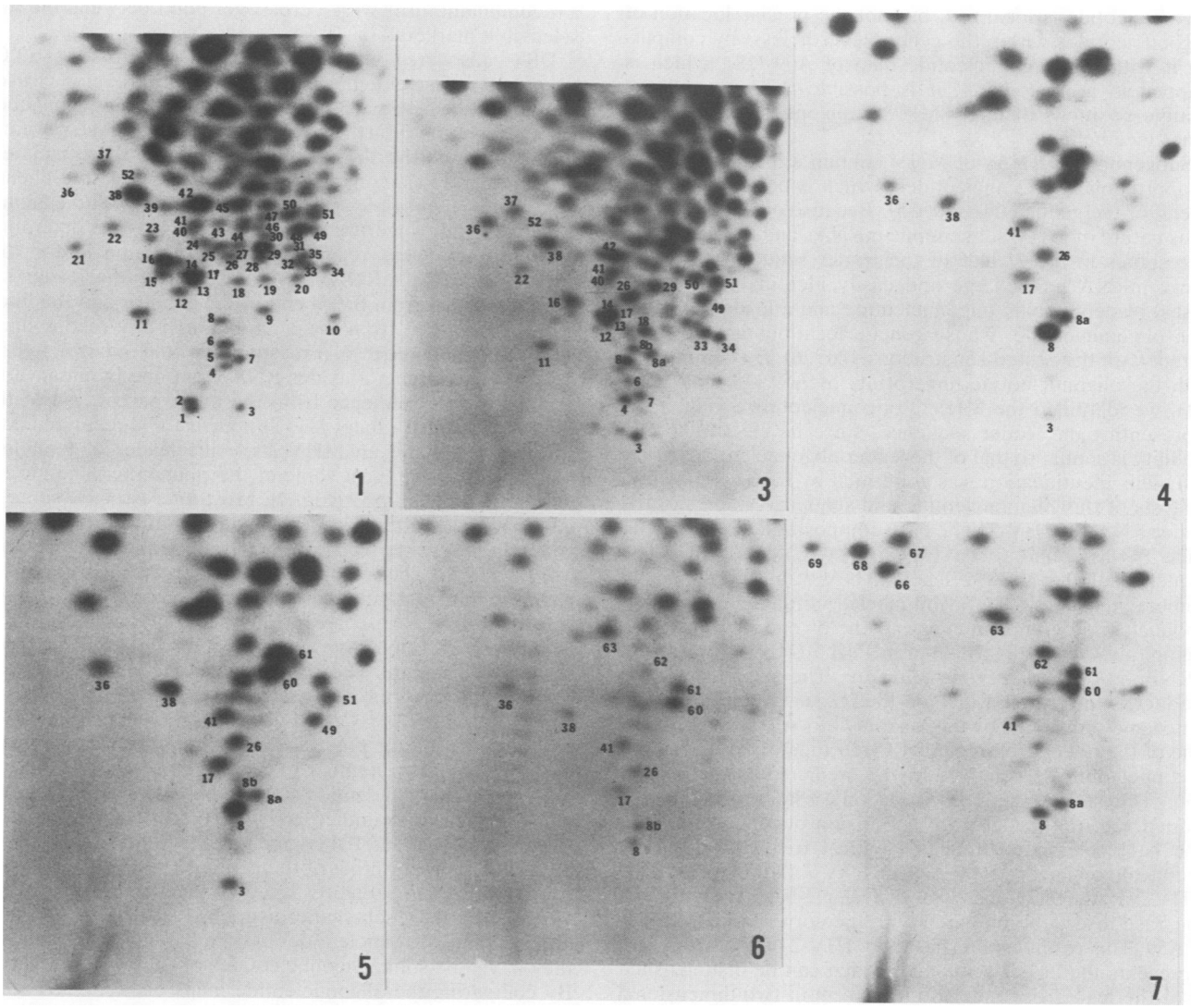


FIG. 1. Oligonucleotide fingerprints of the genomic and subgenomic mRNAs of MHV- 2. Each mRNA species is denoted by a number at the lower right-hand corner of the fingerprint. For instance, 7 denotes mRNA 7. The small numbers in each fingerprint represent arbitrary numbers assigned to each oligonucleotide. Only the large $T_1$ oligonucleotides were studied. Oligonucleotides 8a and 8b are the leader-body fusion sequences of mRNA 7 and mRNA 6, respectively. Their presence in the larger mRNAs was probably due to contamination of smaller mRNAs.

mRNAs (Fig. 1). Since MHV mRNAs have a 3′-coterminal nested-set structure (18), the smallest mRNA 7 represents the sequence of the 3′ end of the genome, and the unique spots in mRNA 6 not present in mRNA 7 represent sequences further to the 5′ side (18). By similar analysis of all of the subgenomic mRNAs in Fig. 1 and the fingerprints of some of the recombinants (see below), a tentative oligonucleotide map was obtained for MHV-2 RNA (Fig. 2). It should be noted that some oligonucleotides, such as oligonucleotides 2, 3, and 6, could not be determined with certainty because of ambiguity in the fingerprints. Also, the relative positions of most of the oligonucleotides within the assigned genes are arbitrary. Therefore, this map could be used only to determine the MHV genes in which a particular

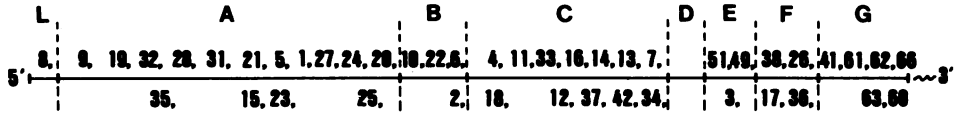


FIG. 2. Schematic oligonucleotide map of MHV-2 RNA genome. The data were derived from Fig. 1. An oligonucleotide was assigned to a specific gene corresponding to the smallest mRNA which contains this oligonucleotide, on the basis of the nested-set structure of MHV mRNAs (18, 31). The numbering of oligonucleotides is the same as in Fig. 1. A through G represent the seven genes of MHV. L represents the leader sequence.

oligonucleotide is localized, but not the precise location of oligonucleotides within the gene. Nevertheless, by comparing it with the oligonucleotide map of A59 (18), which is mapped in greater detail, it is possible to determine the relative positions of many MHV-2 oligonucleotides within genes (see below).

Subgenomic mRNAs of MHV contain a leader sequence of approximately 72 nucleotides, which is derived from the 5′ end of the genome (16, 19, 35). Because of the discontinuous nature of MHV subgenomic mRNAs and the paucity of G residues in the 3′ half of the leader sequence (16, 20), every mRNA has a large and easily identifiable (over 20 bases) leader-specific oligonucleotide and a leader-body fusion oligonucleotide, whose genetic locations are not consistent with the nested-set structure (20, 26). By comparison with the oligonucleotide fingerprints of A59 (18) and JHM (31), we identified the MHV-2 oligonucleotide 8 (Fig. 1) as representing the leader sequence, since its electrophoretic mobility is similar to that of the leader oligonucleotide of A59 (20). This identification was confirmed by base composition analysis of this oligonucleotide and sequence studies of the leader RNA of MHV-2. The base composition of oligonucleotide 8 was found to be $U_{9-10}$ $C_{6-7}(AC)_2(AAAC)G$. The sequence of the MHV-2 leader RNA was determined by primer extension with a 5′-end-labeled synthetic oligodeoxyribonucleotide complementary to the 5′ end of the coding region (nucleotides 84 to 96) of mRNA 7 (1) as a primer and mRNA 7 of MHV-2 as the template. The primer-extended product, which should include the leader region, was then eluted and sequenced by the Maxam-Gilbert method (Fig. 3). One of the underlined regions (#8) in Fig. 3 corresponds to oligonucleotide 8, as judged by the predicted base composition. The second underlined region (#8a) represents the sequence of the leader-mRNA 7 fusion oligonucleotide 8a. The latter oligonucleotide is identical to the leader-body fusion oligonucleotide of A59 mRNA 7 (20). Overall, the MHV-2 leader sequence has five single-base changes and one base insertion compared with the corresponding leader of A59. This result establishes that MHV-2 oligonucleotide 8 represents the leader sequence, which can be distinguished from the leader oligonucleotide of A59 in two-dimensional oligonucleotide fingerprints.

**Isolation of recombinants between MHV-2 and A59.** To isolate recombinants between MHV-2 and A59, we used two genetic markers. The first was the temperature sensitivity of A59 mutant LA7. This virus does not produce virus particles, but synthesizes RNA at the nonpermissive temperature. The second was the cell-cell fusion ability of the viruses: A59 causes cell fusion, whereas MHV-2 does not. Therefore, when cells are infected with both LA7 and MHV-2, any progeny virus which can grow at the nonpermissive temperature and induce cell fusion should represent a recombinant virus with a crossover point between the two selectable markers.

DBT cells were coinfected with these two viruses at 39°C, the nonpermissive temperature for LA7. Progeny viruses were plaque assayed at 39°C, and the fusion-positive plaques were selected and further purified by serial plaque purifications. Early during the purification, two of these isolates, ML-3 and ML-11, converted to the fusion-negative phenotype. All of the isolates were examined by two-dimensional oligonucleotide fingerprinting of their mRNA 7 to determine whether they were recombinants. The rationale for this approach is that mRNA 7 is composed of the leader sequence derived from the 5′ end of the genome and the body sequence derived from the 3′ end. Thus, any recombinant with an odd number of crossovers would have a hybrid mRNA 7 containing a leader RNA from one parental virus and the coding sequence from the other parent. All of the viruses examined except ML-11 appear to be recombinants, since they contain an MHV-2-specific leader oligonucleotide, no. 8, and at least some of the remaining oligonucleotides derived from A59 (Fig. 4). Most interestingly, some of the oligonucleotides within the body of mRNA 7 of ML-3 and ML-8 were derived from A59 and some were derived from MHV-2. This result suggests that these two viruses have a recombination within the 3′-most gene, gene G, of the MHV genome. These are the first recombinants we have ever obtained which have a crossover site in the 3′ end gene of the RNA genome. The only virus which did not seem to be a recombinant virus was ML-11, which has an mRNA 7 identical to that of MHV-2 (Fig. 1). However, this approach does not rule out the possibility that ML-11 is a recombinant virus with an even number of crossovers.

**Genomic characterization of recombinant viruses.** To prove that the viruses examined are indeed recombinants and to determine the sites of recombination, we performed oligonucleotide fingerprinting of the genomic RNAs of these and additional viruses. Figure 5 shows the fingerprints of the viruses and their schematic diagrams. All of these viruses contain some oligonucleotides of both parental origins. Also, they have lost some oligonucleotides of each parental virus. By comparing the oligonucleotide maps of MHV-2 (Fig. 2) and A59 (18), it is possible to determine the approximate sites of recombination (Fig. 6). This result shows that all of the viruses examined, including ML-11, are recombinants. It should be noted that a recombination site is considered established only when oligonucleotides from one parent are present and the corresponding oligonucleotides from the same location on the genome of the other parent are missing. Thus, they represent homologous recombination. Both the fusion-negative recombinants ML-3 and ML-11 have a gene C of MHV-2 origin, whereas the remaining recombinants, all of which are fusion positive, have a gene C with at least

```
                    10          20          30          40          50
A59                   A       U                     C  A       A
MHV-2       UAUAUGAGUG AAUGGCGUCC GUACGUACCC UUUCUACUCU CAAACUCUUG
                                                      #8

                    60          70
A59         -
MHV-2       UUAGUUUAAA UCUAAUCUAA ACUUUAAGG.....................
                       #8a
```

FIG. 3. Leader sequence of MHV-2 RNA. The sequence was obtained by primer extension of a synthetic primer complementary to the 5′ end (nucleotides 84 to 96) of the coding region of mRNA 7 of MHV-2. The extended primer was eluted from the gel and sequenced by the chemical cleavage method (32). The sequence is compared with that of A59 (16). The underlined sequences correspond to the $T_1$ oligonucleotides 8 and 8a in Fig. 1.

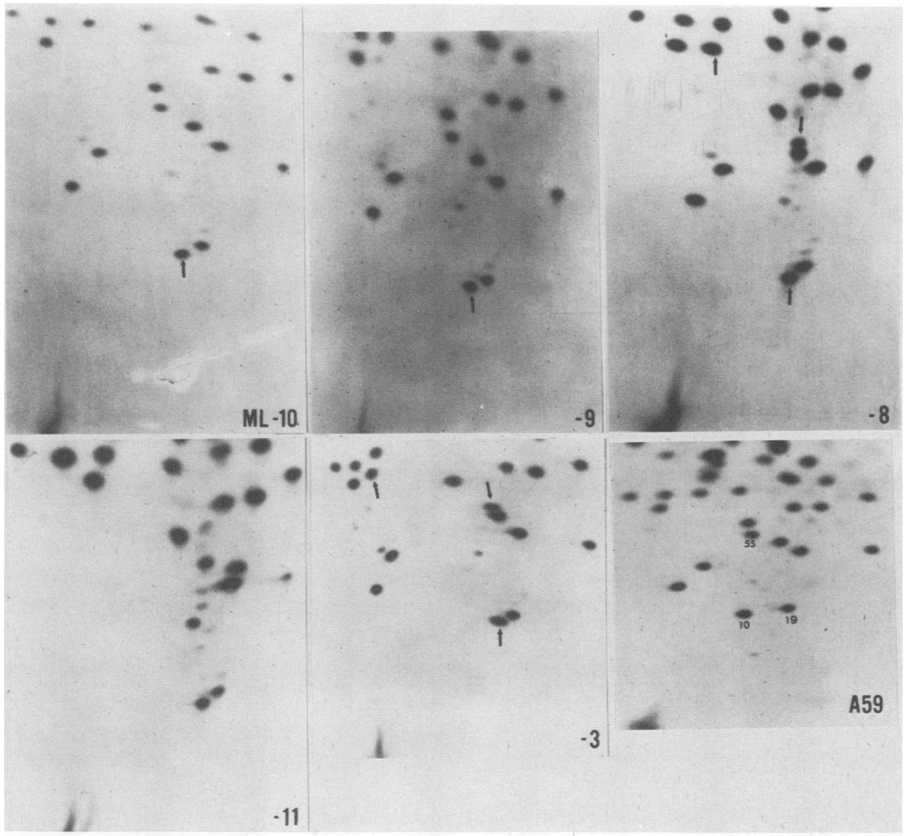


FIG. 4. Oligonucleotide fingerprints of mRNA 7 of different potential recombinant viruses. These fingerprints are compared with that of A59. ML-11 is identical to mRNA 7 of MHV-2 (Fig. 1). The other fingerprints are similar to A59, except for the spots denoted by arrows, which are derived from MHV-2. Oligonucleotide 10 of A59 is derived from the leader region. Oligonucleotide 8 of MHV-2 is the corresponding oligonucleotide derived from the leader region.

some A59 sequences. The details of these maps were further confirmed by studying oligonucleotide fingerprints of subgenomic mRNAs of these recombinants. Since the subgenomic mRNAs are much smaller than the genomic RNA, the oligonucleotide fingerprints are less complex and each oligonucleotide can be more unequivocally discerned. For instance, ML-3 has an mRNA 6 containing all of the A59-specific oligonucleotides unique to gene F (Fig. 7), but an mRNA 5 containing all of the MHV-2-specific oligonucleotides unique to gene E. These data, coupled with the finding that mRNA 7 of ML-3 contains part of the MHV-2-derived sequence and part of the A59-derived sequence (Fig. 4), indicate that ML-3 has two crossover sites located within gene G and at the junction between genes E and F, respectively. Very similar crossover events also occurred in ML-11, except that its recombination sites are localized at the junctions between genes E and F and between genes F and G, respectively. This conclusion is supported by detailed analysis of the fingerprints of the subgenomic mRNAs (data not shown). In addition, both ML-11 and ML-3 probably contain multiple crossovers in gene A, although the presence of the crossovers in gene A of ML-11 is less certain, since only one detectable oligonucleotide was exchanged between the two parental viruses (Fig. 5).

Three additional viruses, ML-7, ML-8, and ML-9 have crossovers within genes B and C (Fig. 6). These recombination sites were confirmed by additional analysis of subgenomic mRNAs 2 and 3 of these viruses (data not shown). Most notably, the 5′ end of gene C sequences was derived from MHV-2, whereas the remaining gene C sequence was from A59. Because the MHV-2 oligonucleotides within gene B could not be mapped with certainty, the crossover sites within gene B of these recombinants were only tentatively mapped, as shown in Fig. 6, which was based on the contiguity of oligonucleotides, thus requiring a minimum number of crossovers.

Several of the recombinants have crossovers in gene A. We have tentatively mapped these crossovers (Fig. 6). Again, because of the uncertainty of the order of oligonucleotides within MHV-2 gene A, we are not certain that the MHV-2 oligonucleotides missing in these recombinants are indeed contiguous. If they are not contiguous, there would be additional crossovers in these recombinants.

These results clearly show that the genetic cross between A59 and MHV-2 produced a variety of RNA recombinants with multiple crossovers. Most notably, recombination in the 3′ end of the genome could also be detected.

**Characterization of structural proteins of recombinants.** Since some of the recombinants have crossovers within the 3′ end genes, which encoded the N and E1 proteins, the structural proteins of these recombinants might reflect the characteristics of both parental viruses. We therefore examined the sizes of their structural proteins. The [$^{35}$S]methionine-labeled intracellular proteins from virus-infected cells were precipitated with a monoclonal antibody which reacts with the N proteins of both A59 and MHV-2 (10) and were separated by polyacrylamide gel electrophoresis (Fig. 8A). Two major N protein species could be detected from each

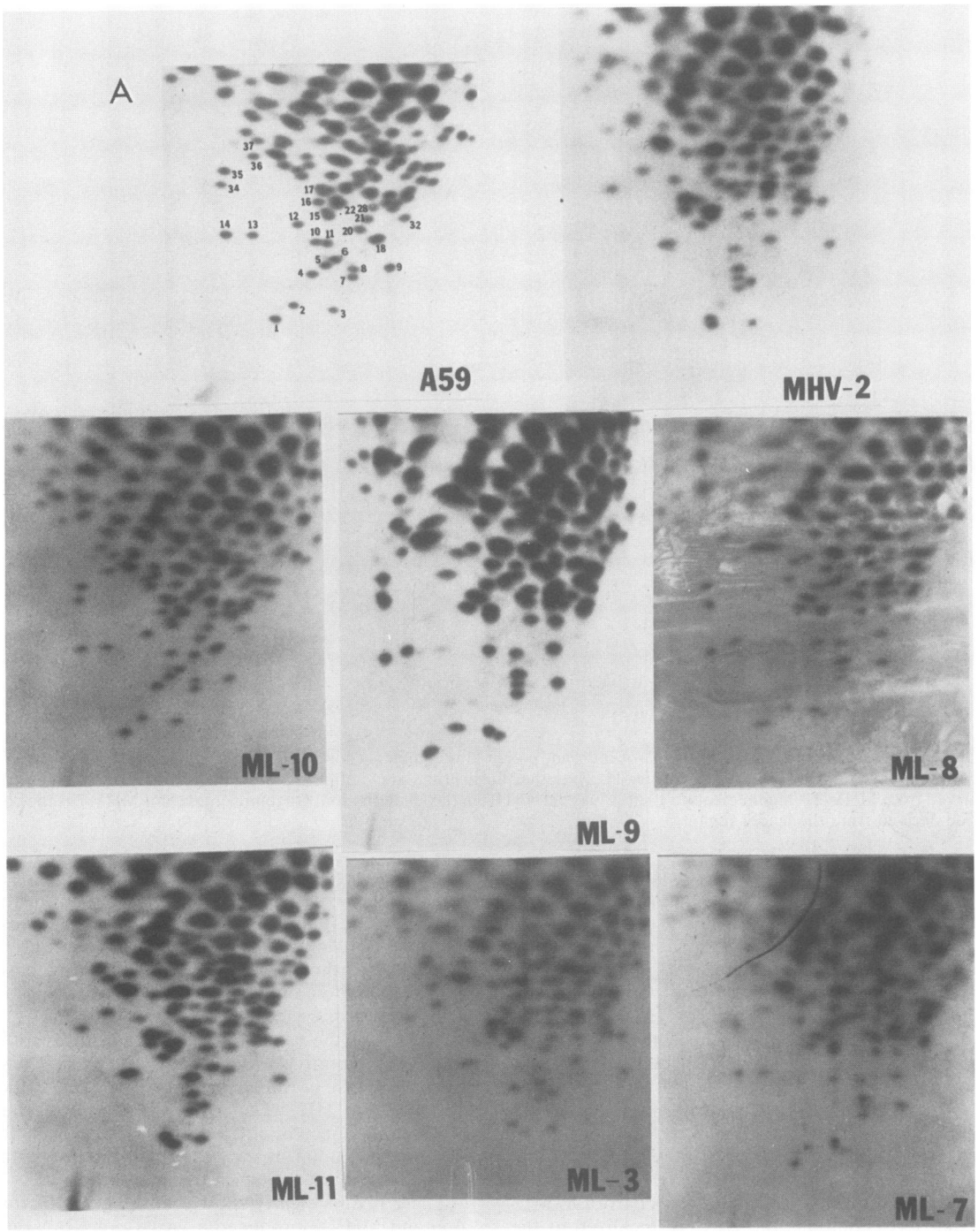


FIG. 5. (A) Oligonucleotide fingerprints of the genomic RNAs of different recombinant viruses and their parental viruses A59 and MHV-2. (B) Schematic diagrams of these fingerprints. Symbols: ●, A59-derived oligonucleotides; ○, MHV-2-derived oligonucleotides.

virus-infected cell. These two protein species probably represent different processed forms of the N protein (33). The sizes of both proteins, particularly the fast-migrating one, are clearly different in MHV-2 and A59. Among the recombinants, ML-11 has an N protein with a size similar to that of MHV-2, whereas ML-7, ML-9, and ML-10 each have an N protein similar to that of A59. Interestingly, the sizes of the N proteins of ML-3 and ML-8 are intermediate between those of the two parental viruses. These protein sizes are in agreement with the genetic structures of these recombinants (Fig. 6). When [$^{35}$S]methionine-labeled virion proteins were analyzed by electrophoresis, a size difference between the E1 of both parents was also seen (Fig. 8B). All of the recombinants examined were found to have an E1 protein with a size like that of A59. Thus, size comparisons of the viral structural proteins N and E1 of recombinants confirmed

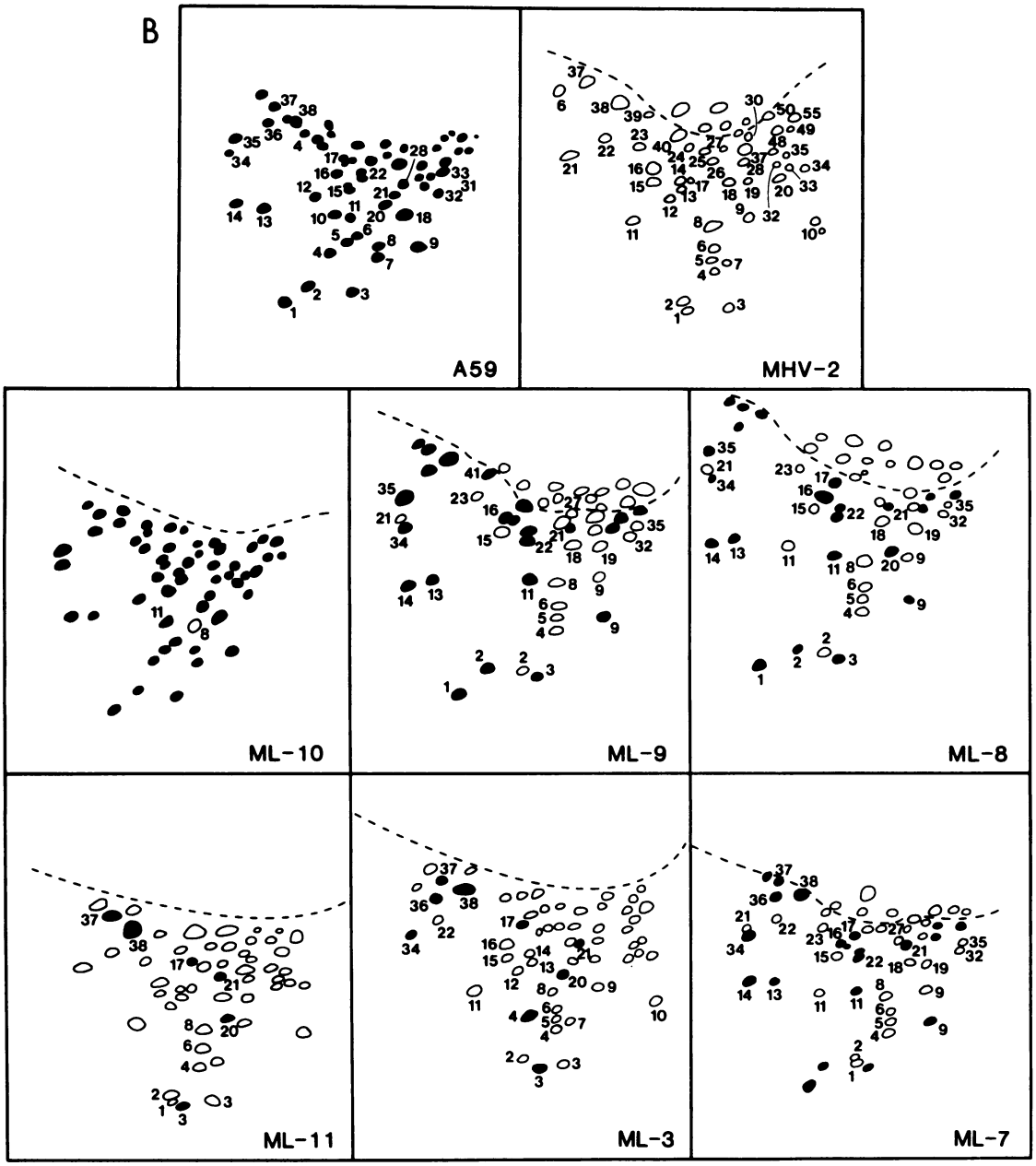


FIG. 5—*Continued.*

the genetic structure of the 3′ ends of these recombinants (Fig. 6).

## DISCUSSION

The data previously presented by researchers in our laboratory (13, 14, 27, 28) and contained in this report show that murine coronaviruses can undergo RNA recombination at a relatively high frequency. This conclusion is supported not only by the presence of a large number of recombinants among the progeny of a single genetic cross (13, 28), but also by the observation that most of the recombinants obtained contain multiple crossovers (13, 27). The multiple crossovers may have resulted from a series of crossing-over events during a single round of RNA replication or during subsequent virus passages. Our observation that some recombinants converted from the fusion-positive to the fusion-negative phenotype during plaque purifications suggests that RNA recombination could continue to occur in every replication cycle. Half of the recombinants obtained between MHV-2 and A59 have crossovers in the 3′ end genes encoding virion structural proteins. There does not seem to be a linkage between the ability of recombinants to induce cell-cell fusion and the parental origin of the 3′ end sequence. Thus, crossovers in this region were most probably not specifically selected for. These recombinational events between MHV-2 and A59 at the 3′ ends of genomic RNA were unexpected, since we have not seen any recombination in this region between A59 and JHM in the approximately 40 different recombinants studied so far (13, 14, 17, 27, 28). It

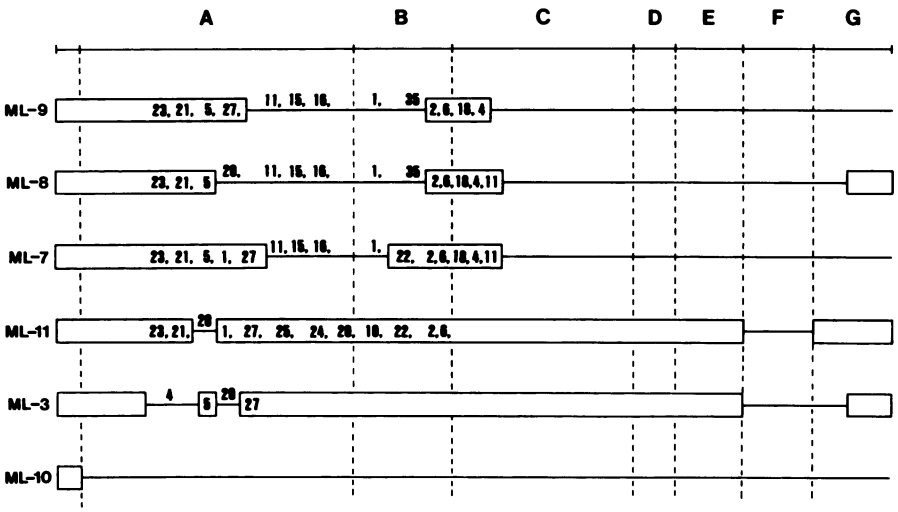


FIG. 6. Genetic maps of the recombinant viruses. Symbols: ——, A59-derived regions; ▭, MHV-2-derived regions. The numbers are the arbitrary numbers assigned to oligonucleotides as shown in Fig. 1 for MHV-2 and as described by Lai et al. (18) for A59. The map is not drawn to scale.

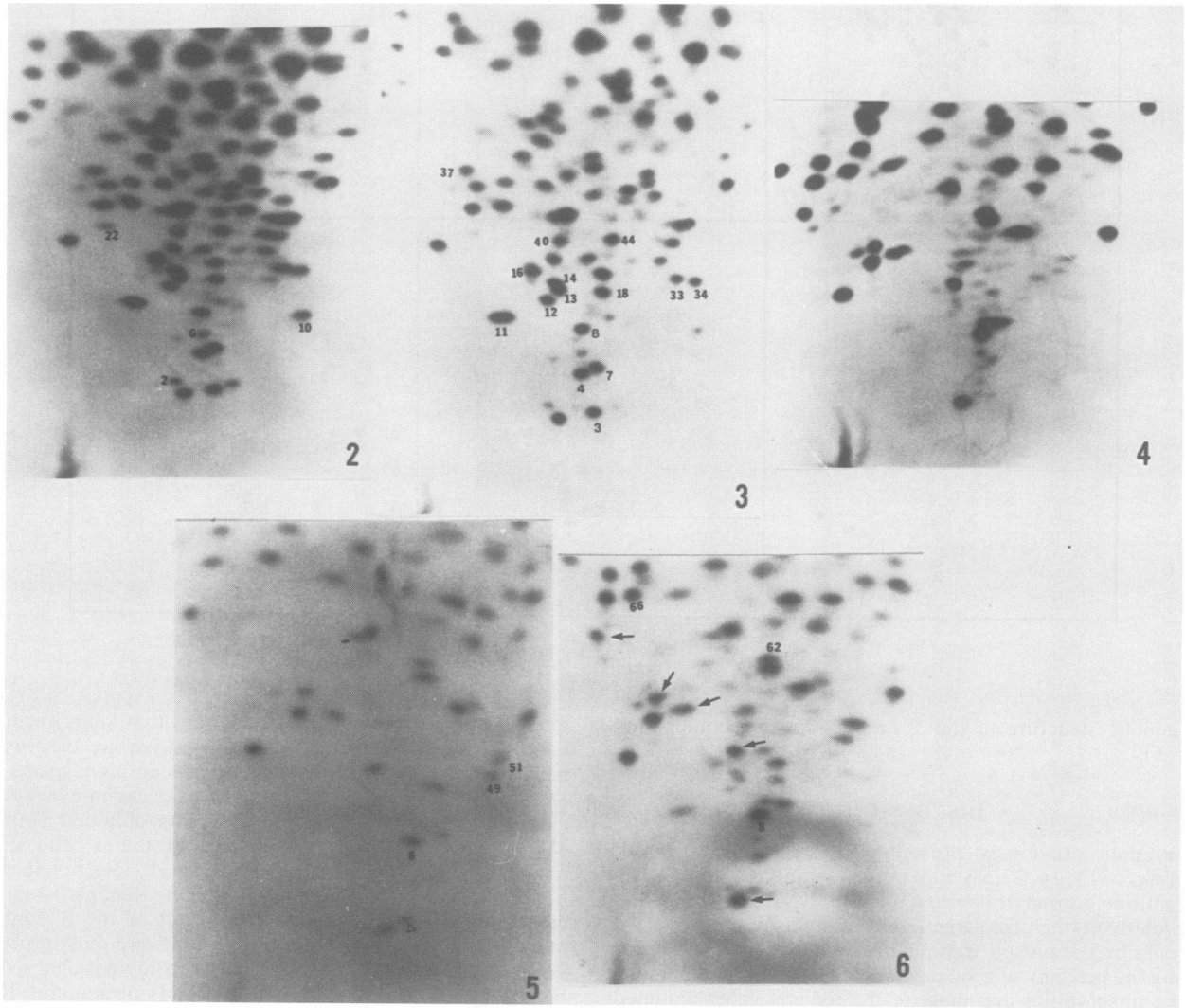


FIG. 7. Oligonucleotide fingerprints of subgenomic mRNAs of ML-3. The numbers at the lower right-hand corners of the fingerprints indicate subgenomic mRNA species. Only the oligonucleotides derived from MHV-2 are numbered. Symbols: △, leader-body fusion oligonucleotide of mRNA 5; ←, oligonucleotides derived from gene F of A59 (18).

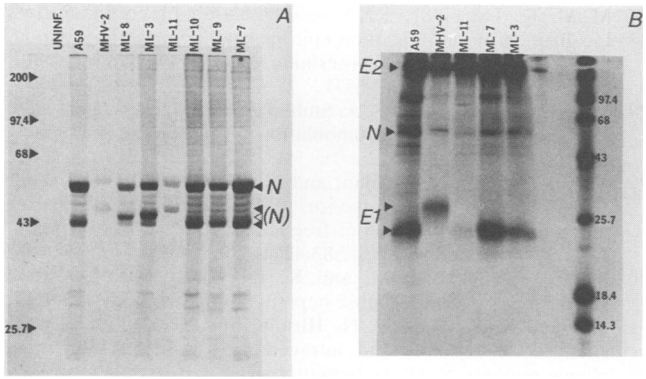


FIG. 8. Polyacrylamide gel electrophoresis of virus-specific proteins of recombinants. (A) The [$^{35}$S]methionine-labeled intracellular N proteins were precipitated with a monoclonal antibody specific for N and separated by polyacrylamide gel electrophoresis (12.5% polyacrylamide). (B) The [$^{35}$S]methionine-labeled virion proteins were electrophoresed on a 12.5% gel. Molecular mass markers are indicated in kilodaltons.

should be noted that the temperature-sensitive mutant LA7 of A59 used in this study has previously been used in other recombination studies (27, 28), which did not yield any recombination events in the 3′ end regions of the genome. It is not clear why the particular genetic cross between LA7 and MHV-2 conducted in this study resulted in many crossovers within this region. Whether the sequence of MHV-2 contributed to the generation of these recombinants remain to be studied.

Among the MHV-2–A59 recombinants obtained, the ability of the virus to induce cell-cell fusion corresponds to the presence of A59-specific sequences at least at the 3′ end of gene C. This finding is consistent with the notion that the peplomer protein (E2) is responsible for the fusion activity of the virus (9, 12, 39). Interestingly, several recombinants have replaced part of the 5′ end of gene C, corresponding to the N terminus of the protein, with MHV-2 sequence. Despite the presence of MHV-2 sequence at the N terminus of the peplomer, these recombinants retain the ability to cause cell-cell fusion. This result suggests, but does not prove, that the portion of the peplomer protein crucial for the fusion activity does not reside in the N terminus. This interpretation is consistent with our previous recombination study which shows that the epitopes of binding of a monoclonal antibody which can inhibit cell fusion reside in the C-terminal half of the peplomer protein (27).

It is interesting that all of the recombinants we have obtained have MHV-2-derived leader sequences. This was not the result of the selection markers used, inasmuch as multiple crossovers occurred throughout the entire genome in most of these recombinants. It is more reasonable to suggest that the MHV-2 leader sequence may have conferred some growth advantages to these recombinants. In DBT cells, MHV-2 appears to grow slightly faster than A59 does. Sequence analysis of the leader region indicates that the MHV-2 leader sequence differs from that of A59 by five single-base changes and one nucleotide insertion (Fig. 3). It is not clear whether these sequence differences are responsible for the altered growth property of the virus. We have previously shown that the A59 leader differs from the JHM leader by a single-base substitution and deletion of a 5-nucleotide (UCUAA) repeat and that A59 grows faster than JHM does. Furthermore, the majority of recombinants between A59 and JHM obtained contain the A59 leader. It would be interesting to determine the leader sequence of additional coronaviruses and compare their growth potentials.

The origin of the ML-10, which contains only leader sequence derived from MHV-2 and the rest of the genome derived from A59, is puzzling. As judged from the previous recombination studies (14), it is unlikely that the temperature-sensitive lesion of LA7 is localized in the leader RNA. Thus, ML-10 must have been derived from recombination between MHV-2 and a revertant of LA7. A similar recombinant was obtained previously between A59 and JHM (14). Although we could not determine the exact site of recombination in these recombinants, the possibility that only the leader sequence is exchanged may suggest that the free leader RNA (2, 4, 29) is involved in the generation of this recombinant.

## ACKNOWLEDGMENTS

We thank Carol Flores for excellent typing of the manuscript.

This work was supported by Public Health Service research grants AI19244 and NS18146 from the National Institutes of Health, by National Multiple Sclerosis Society research grant 1449, and by National Science Foundation grant PCM-4507. L.S.H. was supported by a postdoctoral fellowship from the Bank of America-Giannini Foundation.

## LITERATURE CITED

1. **Armstrong, J., S. Smeekens, and P. Rottier.** 1983. Sequence of the nucleocapsid gene from murine coronavirus MHV-A59. Nucleic Acids Res. **11**:883–891.
2. **Baric, R. S., C.-K. Shieh, S. A. Stohlman, and M. M. C. Lai.** 1987. Analysis of intracellular small RNAs of mouse hepatitis virus: evidence for discontinuous transcription. Virology **156**: 342–354.
3. **Baric, R. S., S. A. Stohlman, and M. M. C. Lai.** 1983. Characterization of replicative intermediate RNA of mouse hepatitis virus: presence of leader RNA sequences on nascent chains. J. Virol. **48**:633–640.
4. **Baric, R. S., S. A. Stohlman, M. K. Razavi, and M. M. C. Lai.** 1985. Characterization of leader-related small RNAs in coronavirus-infected cells: further evidence for leader-primed mechanism of transcription. Virus Res. **3**:19–33.
5. **Barrell, B. G.** 1971. Fractionation and sequence analysis of radioactive nucleotides, p. 751–779. *In* G. L. Cantoni and D. R. Davies (ed.), Procedures in nucleic acid research, vol. 2. Harper & Row, Publishers, Inc., New York.
6. **Brayton, P. R., M. M. C. Lai, C. D. Patton, and S. A. Stohlman.** 1982. Characterization of two RNA polymerase activities induced by mouse hepatitis virus. J. Virol. **42**:847–853.
7. **Brayton, P. R., S. A. Stohlman, and M. M. C. Lai.** 1984. Further characterization of mouse hepatitis virus RNA dependent RNA polymerases. Virology **133**:197–201.
8. **Childs, J. C., S. A. Stohlman, L. Kingsford, and R. Russell.** 1983. Antigenic relationships of murine coronaviruses. Arch. Virol. **78**:81–87.
9. **Collins, A. R., R. L. Knobler, H. Powell, and M. J. Buchmeier.** 1982. Monoclonal antibodies to murine hepatitis virus-4 (strain JHM) define the viral glycoprotein responsible for attachment and cell-cell fusion. Virology **119**:358–371.
10. **Fleming, J. O., S. A. Stohlman, R. C. Harmon, M. M. C. Lai, J. A. Frelinger, and L. P. Weiner.** 1983. Antigenic relationships of murine coronavirus: analysis using monoclonal antibodies to JHM (MHV-4). Virology **131**:296–307.
11. **Hirano, N., K. Fujiwara, S. Hino, and M. Matsumoto.** 1974. Replication and plaque formation of mouse hepatitis virus (MHV-2) in mouse cell line DBT culture. Arch. Gesamte Virusforsch. **44**:298–302.
12. **Holmes, K. V., E. W. Doller, and J. N. Behnke.** 1981. Analysis of the functions of coronavirus glycoproteins by differential

inhibition of synthesis with tunicamycin. Adv. Exp. Med. Biol. **142**:133–142.
13. **Keck, J. G., G. K. Matsushima, S. Makino, J. O. Fleming, D. M. Vannier, S. A. Stohlman, and M. M. C. Lai.** 1988. In vivo RNA-RNA recombination of coronavirus in mouse brain. J. Virol. **62**:1810–1813.
14. **Keck, J. G., S. A. Stohlman, L. H. Soe, S. Makino, and M. M. C. Lai.** 1987. Multiple recombination sites at the 5′-end of murine coronavirus RNA. Virology **156**:331–341.
15. **Laemmli, U. K.** 1970. Cleavage of structural proteins during the assembly of the head of bacteriophage T4. Nature (London) **227**:680–685.
16. **Lai, M. M. C., R. S. Baric, P. R. Brayton, and S. A. Stohlman.** 1984. Characterization of leader RNA sequence on the virion and mRNAs of mouse hepatitis virus, a cytoplasmic virus. Proc. Natl. Acad. Sci. USA **31**:3626–3630.
17. **Lai, M. M. C., R. S. Baric, S. Makino, J. G. Keck, J. Egbert, J. L. Leibowitz, and S. A. Stohlman.** 1985. Recombination between nonsegmented RNA genomes of murine coronaviruses. J. Virol. **56**:449–456.
18. **Lai, M. M. C., P. R. Brayton, R. C. Armen, C. D. Patton, C. Pugh, and S. A. Stohlman.** 1981. Mouse hepatitis virus A59: mRNA structure and genetic localization of the sequence divergence from hepatotropic strain MHV-3. J. Virol. **39**:823–834.
19. **Lai, M. M. C., C. D. Patton, R. S. Baric, and S. A. Stohlman.** 1983. Presence of leader sequences in the mRNA of mouse hepatitis virus. J. Virol. **46**:1027–1033.
20. **Lai, M. M. C., C. D. Patton, and S. A. Stohlman.** 1982. Further characterization of mRNAs of mouse hepatitis virus: presence of common 5′ end nucleotides. J. Virol. **41**:557–565.
21. **Lai, M. M. C., C. D. Patton, and S. A. Stohlman.** 1982. Replication of mouse hepatitis virus: negative-stranded RNA and replicative form RNA are of genome length. J. Virol. **44**: 487–492.
22. **Lai, M. M. C., and S. A. Stohlman.** 1978. RNA of mouse hepatitis virus. J. Virol. **26**:235–242.
23. **Lai, M. M. C., and S. A. Stohlman.** 1981. Comparative analysis of RNA genomes of mouse hepatitis viruses. J. Virol. **38**:661–670.
24. **Langridge, L., P. Langridge, and P. L. Berquist.** 1980. Extraction of nucleic acids from agarose gels. Anal. Biochem. **103**:264–271.
25. **Leibowitz, J. L., S. R. Weiss, E. Paavola, and C. W. Bond.** 1982. Cell-free translation of murine coronavirus RNA. J. Virol. **43**: 905–913.
26. **Leibowitz, J. L., K. C. Wilhelmsen, and C. W. Bond.** 1981. The virus-specific intracellular RNA species of two murine coronavirus: MHV-A59 and MHV-JHM. Virology **114**:39–51.
27. **Makino, S., J. O. Fleming, J. G. Keck, S. A. Stohlman, and M. M. C. Lai.** 1987. RNA recombination of coronaviruses: localization of neutralization epitopes and neuropathogenic determinants on the carboxyl-terminus of peplomers. Proc. Natl. Acad. Sci. USA **84**:6567–6571.
28. **Makino, S., J. G. Keck, S. A. Stohlman, and M. M. C. Lai.** 1986. High-frequency RNA recombination of murine coronaviruses. J. Virol. **57**:729–737.
29. **Makino, S., S. A. Stohlman, and M. M. C. Lai.** 1986. Leader sequences of murine coronavirus mRNAs can be freely reassorted: evidence for the role of free leader RNA in transcription. Proc. Natl. Acad. Sci. USA **83**:4204–4208.
30. **Makino, S., F. Taguchi, and K. Fujiwara.** 1984. Defective interfering particles of mouse hepatitis virus. Virology **113**:9–17.
31. **Makino, S., F. Taguchi, N. Hirano, and K. Fujiwara.** 1984. Analysis of genomic and intracellular viral RNAs of small plaque mutants of mouse hepatitis virus, JHM strain. Virology **139**:138–151.
32. **Maxam, A. M., and W. Gilbert.** 1980. Sequencing end-labeled DNA with base-specific chemicals cleavages. Methods Enzymol. **65**:499–560.
33. **Robbins, S. G., M. F. Frana, J. J. McGowan, J. F. Boyle, and K. V. Holmes.** 1986. RNA-binding proteins of coronavirus MHV: detection of monomeric and multimeric N protein with an RNA overlay-protein blot assay. Virology **150**:402–410.
34. **Rottier, P. J. M., W. J. M. Spaan, M. Horzinek, and B. A. M. van der Zeijst.** 1981. Translation of three mouse hepatitis virus (MHV-A59) subgenomic RNAs in *Xenopus laevis* oocytes. J. Virol. **38**:20–26.
35. **Spaan, W., H. Delius, M. Skinner, J. Armstrong, P. Rottier, S. Smeekens, B. A. M. van der Zeijst, and S. G. Siddell.** 1983. Coronavirus mRNA synthesis involves fusion of non-contiguous sequences. EMBO J. **2**:1939–1944.
36. **Stohlman, S. A., and M. M. C. Lai.** 1979. Phosphorproteins of murine hepatitis viruses. J. Virol. **32**:672–675.
37. **Sturman, L. S.** 1977. Characterization of a coronavirus. I. Structural proteins: effects of preparative conditions on the migration of proteins in polyacrylamide gels. Virology **77**:637–649.
38. **Sturman, L. S., and K. V. Holmes.** 1977. Characterization of a coronavirus. II. Glycoproteins of the viral envelope: tryptic peptide analysis. Virology **77**:650–660.
39. **Sturman, L. S., and K. V. Holmes.** 1984. Proteolytic cleavage of peplomeric glycoprotein E2 of MHV yields two 90K subunits and activates cell fusion. Adv. Exp. Med. Biol. **173**:25–35.
40. **Sturman, L. S., K. V. Holmes, and J. Behnke.** 1980. Isolation of coronavirus envelope glycoproteins and interaction with the viral nucleocapsid. J. Virol. **33**:449–462.
41. **Wege, H., A. Muller, and V. ter Meulen.** 1978. Genomic RNA of the murine coronavirus JHM. J. Gen. Virol. **41**:217–227.